Environmental Science and Pollution Research
https://doi.org/10.1007/s11356-019-05495-2

SUSTAINABLE INDUSTRIAL AND ENVIRONMENTAL BIOPROCESSES

Potentiometric polyphenol oxidase biosensor for sensitive determination of phenolic micropollutant in environmental samples

Shivamurthy Ravindra Yashas[1] · Shadakshari Sandeep[2] · Ballagere Puttaraju Shivakumar[1] · Ningappa Kumara Swamy[2]

Received: 29 January 2019 / Accepted: 15 May 2019

Abstract

The present study demonstrates the development of polyphenol oxidase (PPO) biosensor for the detection of catechol using strontium copper oxide ($SrCuO_2$) and polypyrrole nanotubes (PPyNT) matrix. The $SrCuO_2$ micro-seeds, a perovskite compound, are synthesized by co-precipitation under pH 8.0. The as-synthesized micro-seeds are characterized by scanning electron microscopy (SEM), field emission scanning electron microscopy (FE-SEM), energy-dispersive X-ray spectroscopy (EDX), and X-ray diffraction spectroscopy (XRD). The proposed sensor is fabricated on pencil graphite (P-Gr) by successive deposition of PPyNT, $SrCuO_2$, and PPO enzyme. The developed PPO/$SrCuO_2$/PPyNT/P-Gr sensor is characterized by cyclic voltammetry (CV), differential pulse voltammetry (DPV), and electrochemical impedance spectroscopy (EIS) techniques. The PPO/$SrCuO_2$/PPyNT/P-Gr displayed excellent electrocatalytic activity towards the oxidation and detection of catechol. The as-developed sensor showed sensitive response ascribing to limit of detection (LOD) of 0.15 μM and sensitivity of 15.60 μA μM^{-1} cm^{-2}. The fabricated sensor exhibited excellent repeatability and longer shelf life. The proposed biosensor finds its application within the broad linear range of 1–50 μM. Real sample analysis of mineral water, tap water, and domestic wastewater using developed sensor showed acceptable recovery. Hence, the biosensor endeavors its application in environmental monitoring and protection.

Keywords Catechol · Strontium copper oxide · Biosensor · Polyphenol oxidase · Pencil graphite electrode

Introduction

There is ubiquitous use of the vital phenolic derivative, catechol, for various industrial applications such as in refineries, pharmaceuticals, rubber, plastics, dyestuffs, pesticides, textile mills, tanning etc. (Wang et al. 2013; Yan et al. 2016; Liu et al. 2019) causing environmental pollution. In addition, catechol is an important metabolite formed by the degradation of organic pollutants (Liu et al. 2019). Catechol has well-established pernicious effects even at nanogram concentrations in environmental samples such as air, water, wastewater etc. The International Agency for Research on Cancer has categorized catechol in group 2B concerning its carcinogenicity (Khorsandi et al. 2018). US Environmental Protection Agency, as well as European Commission, has listed phenol and its derivatives under the list of priority pollutants to carefully monitor them (Yogita et al. 2016). The catechol seeps into the food chain mainly through the water or wastewater source inducing adverse health effects on aquatic fauna and humans. The direct impact on the respiratory system, genital-urinary system, liver, kidney etc. due to its persistent toxicity is well reported (Fartas et al. 2017). Thus, research on developing a simple, economical, and reliable technique to quantify catechol in wastewater is the need of the hour.

The various spectrophotometric and chromatographic techniques are conventionally employed to detect and quantify phenolic derivatives in environmental samples (Yashas et al. 2018). Eventually, the development of electrochemical biosensors has received core attention in recent years because of numerous advantages over existing techniques like high-performance liquid chromatography, surface plasmon resonance spectroscopy, quartz crystal microbalance, and electrophoresis (Zhu et al. 2014). Though classical methods output

Responsible editor: Bingcai Pan

✉ Ningappa Kumara Swamy
kumaryagati@gmail.com

[1] Department of Environmental Engineering, JSS Science and Technology University, Mysuru, Karnataka 570006, India

[2] Department of Chemistry, JSS Science and Technology University, Mysuru, Karnataka 570006, India

Published online: 27 May 2019

accurate and precise results, they are notably costly, laborious, involves critical and precise operations, lack sensitivity, involves pre-treatment of sample, large instrumentations etc. (Zeng et al. 2016; Arfin and Rangari 2018; Sandeep et al. 2018b). The merits of an enzyme-based electrochemical biosensor as a bio-analytical tool has flourished and challenged the conventional methods attributing to its rapid response, no pre-treatment of samples, economical, excellent selectivity, sensitivity, storage-stability, reproducibility, and low detection limits (Nandini et al. 2014; Swamy et al. 2017; Arfin and Rangari 2018; Sandeep et al. 2018b; Yashas et al. 2018).

The present study engages PPO as biorecognition element, which is a gifted multi-copper containing oxidoreductase class of enzyme copiously found in fruits and vegetables responsible for browning and show high catalytic activity for most phenolic substrates (de Lima et al. 2010). The special ability of PPO to catalyze electron transfer reactions in absence of any co-factors makes it promising for construction of biosensors (Gul et al. 2017). In the present study, PPO enzyme is extracted from Sweet Potato (*Ipomoea batatas)*.

Appropriate enzyme immobilization method is important to ensure intimate contact of the bioreceptor with the transducer for effective signal transduction. Adsorption stands out to be simple, rapid, and widely applied one in fabricating most of the PPO-based electrochemical biosensors, and it is implemented in the present study.

The transducer matrix is an integral part of a biosensor. The lesser-known perovskite, $SrCuO_2$, is exploited for its catalytic behavior towards catechol as one of the transducer element. The alkaline-metal-doped, transition metal-oxide is presumed to be a potential transducer candidate by the combined influence of strontium (Sr) and copper oxide (CuO). CuO is one of the highly efficient catalysts known for its large surface area (Han et al. 2006). Sr imparts its dielectric and tunable properties to form a large number of semiconductor and superconductor complexes, and Sr-doped with metal oxides are reported to display high catalytic traits (Han et al. 2006; Yousefi et al. 2015; Aziz et al. 2012). In addition, with the perovskite material, PPyNT is used to create a better matrix to house the enzyme that would enhance the biorecognition of the sensor. Li et al. (2017) inferred on the environmental stability and the biocompatibility of PPyNT for biosensing applications. Furthermore, the results confirmed about the longevity of sensor response and efficient electron transfer property of the new matrix. Altogether, PPyNT/$SrCuO_2$ constitutes the transduction system of the proposed sensor.

The present study proposes enzyme/micro-perovskite/polypyrrole nanotube-modified pencil graphite (PPO/$SrCuO_2$/PPyNT/P-Gr) bioelectrode for catechol quantification, which is unexplored to date. The details of synthesis and characterization of $SrCuO_2$ and PPyNT, extraction and assay of PPO from sweet potato, modification of P-Gr, electrode characterization and calibration, determination of liner range, limit of detection (LOD) and sensitivity of sensor, storage-stability and reproducibility study, and the practical applicability of the as-modified electrode is presented.

Materials and methods

Chemicals and equipment

The P-Gr is from Hindustan Pencils Private Limited, Mumbai, India, sold under the brand name *Apsara Platinum Extra Dark*. The quality of the pencil confirms to 2B type. Chemicals, namely, strontium nitrate ($Sr(NO_3)_2$), copper(II) nitrate hemihydrate ($Cu(NO_3)_2{\cdot}5H_2O$), sodium hydroxide (NaOH), pyrrole monomer (C_4H_5N), ferric chloride hexahydrate ($FeCl_3$. $6H_2O$), methyl orange ($C_{14}H_{14}N_3NaO_3S$), sodium dihydrogen phosphate, disodium hydrogen phosphate, and potassium chloride (KCl) are procured from Sigma Aldrich and Fischer Scientific. Shimadzu Europa GmbH, UV-visible spectrophotometer, UV-1800, is used for spectral measurements. Proto Manufacturing Inc., XRD, benchtop powder diffractometer, is used to record crystallographic information using Cu K-Alpha radiation as a source ($\lambda =$ 0.15443 nm). Morphological studies are carried out using a scanning electron microscope, JSMIT300 (JEOL, Singapore); the field emission scanning electron microscope, JSM-7100F (JEOL, Singapore); and the Brunauer–Emmett–Teller(BET) analysis with BELSORP-max (MicrotracBEL, Japan).

Extraction of PPO enzyme

The PPO enzyme is crudely extracted from *Ipomoea batatas*. The extraction protocol and the assay are performed similarly to that reported by Sandeep et al. (2018a, b). In brief, 25 g of fruit pulp is homogenized with 25 ml of 0.05 M phosphate buffer (PBS) of pH 6.8, 1% polyvinyl pyrrolidone, 1% Triton X-100 and 1 mM phenyl-methyl-sulfonyl-fluoride (PMSF) for 10 min. The homogenate is rapidly filtered and centrifuged at 10,000 rpm for 15 min in 4 °C. The PPO activity is determined spectrophotometrically using 4-methyl catechol as substrate. Enzyme assay is carried out by taking 0.88 ml of PBS (pH 6.8, 50 mM) and 0.02 ml of enzyme extract with 0.1 ml of catechol as substrate (0.1 M). The increase in absorbance at 420 nm is monitored for 3 min using a spectrophotometer, and the average change in absorbance per minute is calculated. As no increase in absorbance is observed for tyrosinase as a substrate, the extracted enzyme lacked monophenolase activity but confirms catecholase activity. The enzyme activity is found to be 20.52 enzyme Unit/mL of crude extract. The extract is stored under 4 °C in a refrigerator and used as a PPO source for further experiments.

Synthesis of $SrCuO_2$ and PPyNT

An equal volume of 0.05 M $Sr(NO_3)_2$ is coupled with 0.1 M of $Cu(NO_3)_2 \cdot 5\ H_2O$ solution to obtain a homogeneous blue mixture. Then, the pH is altered to 8 with 0.1 M NaOH and stirred for about 3 h at 80 °C to obtain a dark blackish-blue colored solution. The solution is centrifuged (10,000 rpm for 10 min), and the precipitate is washed with a copious amount of double-distilled water and ethanol. The obtained filtrate is dried at 80 °C in a hot air oven and finally calcinated at 600 °C for 2 h in a muffle furnace to get powdered $SrCuO_2$.

PPyNT is grown from methyl orange as a template as followed by Li et al. (2017). In summary, 105 μL (1.5 mM) of pyrrole monomer is added to 30 mL of 5 mM methyl orange. Then, 0.406 g (1.5 mM) of $FeCl_3 \cdot 6H_2O$ is added till a precipitate is formed. The reaction mixture is stirred at 25 °C for 24 h. The PPyNT precipitate is washed with ethanol/deionized water several times until filtrate is neutral and colorless. Finally, the precipitate is oven dried (60 °C for 24 h) to obtain the PPyNT.

Fabrication of PPO/$SrCuO_2$/PPyNT/P-Gr electrode

The P-Gr is obtained from the 2B pencil by skinning off the wooden portion and polishing its tip using PK-3 electrode polishing kit (0.05 μm aqueous polishing alumina and 1 μm polishing diamond) till a shining surface is obtained. The polished electrode surface is washed with distilled water and methanol, and then sonicated to remove loosely bound fragments from the electrode surface. The P-Gr electrode is modified by depositing 1.5 μL aliquot of PPyNT (2 mg/mL of deionized water) and dried. The resulting PPyNT/P-Gr electrode is further modified by drop-casting 0.8 μL aliquot of $SrCuO_2$ (6 mg/mL of deionized water) and dried. The resulting $SrCuO_2$/PPyNT/P-Gr electrode is further modified by depositing 2 μL of crude PPO extract and dried thoroughly to obtain PPO/$SrCuO_2$/PPyNT/P-Gr working electrode. The as-developed sensor is stored at 4 °C until used in further studies.

Electrochemical studies

The electrochemical studies are carried out employing electrochemical workstation SP-150 of Bio-Logic Science Instruments, France. The data analysis is carried out with the EC-Lab® software package. The traditional three-electrode configuration electrochemical cell is used for the study in which saturated calomel electrode (SCE) is the reference, platinum wire served as the counter electrode and modified P-Gr as working electrode. The techniques such as CV, DPV, and EIS are employed in the present study to characterize, optimize, and calibrate the developed sensor. The electrochemical investigations of bare and modified P-Gr are performed in PBS (pH 7.0) containing 5 mM $[Fe(CN)_6]^{-3/-4}$ as an electrochemical probe. EIS measurements in the frequency range of 100 kHz to 0.1 Hz are performed to study the charge transfer process at electrode/electrolyte interface.

Results and discussion

Characterization of $SrCuO_2$ by SEM, FE-SEM, EDX, and XRD

The as-obtained $SrCuO_2$ powder is first subjected to SEM and FE-SEM to study morphology. The SEM image is captured by accelerating 15.0 kV at × 6000 magnification. Similarly, FE-SEM is the image captured by accelerating 10.0 kV LED at × 20,000 magnification. Figure 1a and b present the SEM and FE-SEM micrographs respectively. The formation of nearly rhombic micro-seeds is evident. Clustered seeds are observed in each of the pictures.

The micro-seeds are then studied with EDX to know the elemental composition. Figure 1 c shows the EDX plot. The plot shows intense peaks corresponding to elements bound to K shell, L shell, and K shell of oxygen, strontium, and copper respectively. Specifically, it informs about the percentage by weight of the element by which it is present in the sample and corresponding atomic percentage of the element. The sample contains 51.01% of strontium, 40.74% of oxygen, and 8.25% of copper by their weight and corresponding atomic percent of 78.15% oxygen, 17.87% strontium, and 3.98% copper. Since no other trace elements are present in the sample, the as-synthesized material is ultra-pure.

The crystallographic information is obtained using powder diffractometer, which used Cu K-Alpha radiation as a source. The 2θ angular regions between 10° and 80° are explored at a scan rate of 2°/min. The XRD pattern is as shown in Fig. 1d. The intense peaks are prominent between 20° and 50° in the pattern. Specifically, the maximum peak is registered at different 2θ, namely, 32.15, 35.50, 38.66, 48.78, 53.33, 58.29, 61.40, 66.24, 67.91, and 75.02. The peak positions and peak intensities obtained are comparable with the reference XRD pattern JCPDS Card No. 00-038-1179 and also reported by Balasubramanian et al. 2017. This suggests that the material is crystalline nature and suits to be a transducer for the sensor.

Characterization of PPyNT by FE-SEM

The synthesized PPyNTs are subjected to FE-SEM to know its physical traits. Figure 1 e depicts the tubular structured PPyNT. The micrograph is captured at × 15,000 magnification by accelerating voltage of 10.0 kV LED. The tubes possess a larger surface area and form a favorable matrix to house the enzyme and thoroughly bind the micro-seeds onto the electrode surface. The as-synthesized pyrrole nanotubes display

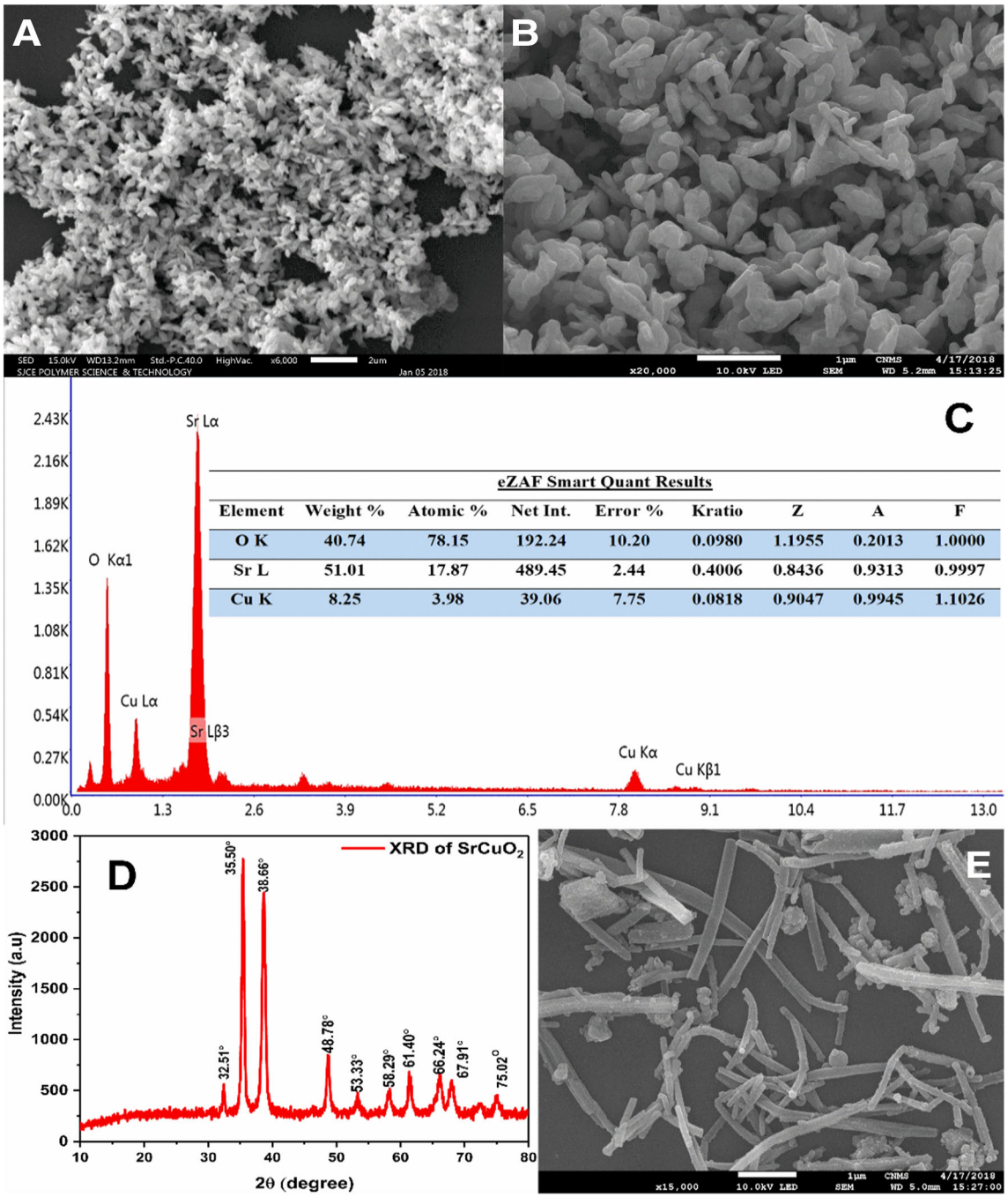

Fig. 1 **a** SEM and **b** FE-SEM of $SrCuO_2$ micro-seeds. **c** EDX spectra of $SrCuO_2$; inset is the elemental quantity results obtained from EXD. **d** XRD pattern of $SrCuO_2$. **e** FE-SEM of PPyNT

similar characteristics reported by Yang et al. (2005); Kopecky et al. (2012); and Li et al. (2017). In order to explore the tubular characteristics, BET analysis is carried out. The PPyNT possess 54.212 $m^2\ g^{-1}$ specific surface area, 0.062621 $cm^3\ g^{-1}$ total pore volume, and 4.6205 nm mean pore diameter. The high specific surface area along with rational pore volume mark the PPyNT more reliable to enhance conductivity for sensing applications (Kopecký et al. 2017; Trchová and Stejskal 2018).

Physical characterization of modified P-Gr by SEM

The deposition of PPO, $SrCuO_2$, and PPyNT on P-Gr is used as the working probe. SEM ascertains the physical entities of the modified electrode as shown in Fig. 2. The SEM image is captured by accelerating 10.0 kV of probe current at × 3000 magnification. Figure 2 demarks SEM micrograph of PPyNT, $SrCuO_2$ micro-seeds, and PPO enzyme respectively. SEM image shows the successful deposition of the nanomaterials and

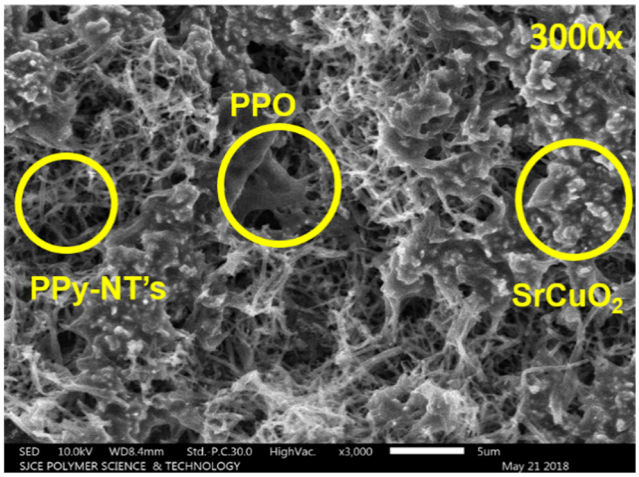

Fig. 2 SEM of PPO/$SrCuO_2$/PPyNT/P-Gr electrode

protein on the surface of P-Gr. The micrographs also show that the deposition of the nanomaterials increases active surface area for biorecognition.

Electrochemical characterization of the modified electrode

EIS characterizes the modified electrode by measuring the charge transfer resistance (R_{ct}) from best-fit Randles electrical equivalent circuit. The EIS is recorded in 0.1 M PBS (pH 7.0) containing 1 mM $[Fe(CN)_6]^{4-/3-}$. All impedance measurements are conducted at the assigned potential of the redox probe at an amplitude of 5 mV and between 100 kHz and 0.1 Hz frequency range. EIS data is presented for each modification of the electrode, bare P-Gr, PPyNT/P-Gr, $SrCuO_2$/PPyNT/P-Gr, and PPO/$SrCuO_2$/PPyNT/P-Gr and is represented in Fig. 3 as a Nyquist diagram. The R_{ct} for P-Gr/PPyNT (4.792 kΩ) is less than bare P-Gr (13.178 kΩ) because of poor electron transportability of the bare electrode. In contrast, the introduction of PPyNT has increased electroactive sites resulting in increased electrochemical activity. Thereafter, the addition of $SrCuO_2$ record least R_{ct} of 2.013 kΩ due to a high rate of electron transfer between nanomaterials and the redox probe. Finally, PPO increased the R_{ct} nearly threefold that is due to the insulating property of enzymes (5.832 kΩ) resulting delay in the electroactivity. This dramatic variation authenticates the immobilization of enzyme and assumes that the same can be a good sensing platform. In addition, the linear portion of the plots obtained infer on the diffusion controlled process at the electrode/electrolyte interface (Maringa et al. 2013; Usai et al. 2019).

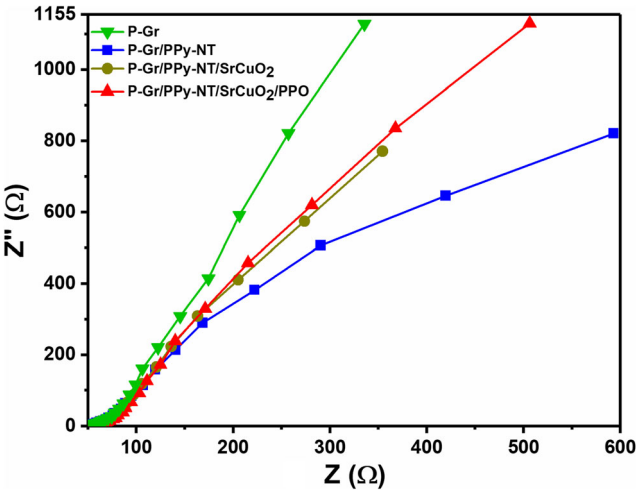

Fig. 3 Nyquist relationships of EIS data of P-Gr, PPyNT/P-Gr, $SrCuO_2$/PPyNT/P-Gr, and PPO/$SrCuO_2$/PPyNT/P-Gr electrodes

Effect of pH, scan rate, and voltammetric response of modified bioelectrode

As an operating parameter, pH influences the signal response and the effect of pH in different pH conditions is studied by CV. The CV is recorded in PBS for pH ranging from 3 to 9 in presence of 10 μM catechol. The plot of oxidation peak currents as a function of different pH is as in Fig. 4a. The highest current (0.118 mA) is recorded at pH 7.0 which is because of highest activity of PPO enzyme resulting in efficient catalytic activity towards the catechol. Hence, the pH 7 is considered as optimum for further electrochemical investigations.

The sensor is scrutinized for scan rate from 25 mV/s to 250 mV/s in the presence of 10 μM catechol in 0.1 M PBS (pH = 7.0) using CV. The potential sweep is fixed from − 0.4 V to 0.8 V. Figure 4 b shows the resultant voltammogram. The graph indicates the proportional increase in the redox peaks with increasing scan rate. In other words, an increase of anodic (oxidation) peak and cathodic (reduction) peak respectively. This is attributed to the larger surface area contributing to faster electron transferability. The relation between the oxidation and reduction current and the square root of scan rate is established in the inset of Fig. 4b. The linear anodic and cathodic peak current as a function of the root of scan rate has $R^2 = 0.9980$ that underscores best-fit obeying Sevcik relation as remarked by David et al. (2013). This claims the mechanism at the P-Gr interface is a diffusion-controlled electrocatalytic process.

The CV is recorded to evaluate the behavior of each modified electrode for detection of catechol in the potential range − 0.4 V to 0.8 V in presence of 10 μM of catechol in 0.1 M PBS (pH = 7), and at the scan rate of 50 mV/s. Figure 4 c represents a plot of the current versus the potential under the above conditions for the electrodes P-Gr, PPyNT/P-Gr, $SrCuO_2$/PPyNT/P-Gr, and PPO/$SrCuO_2$/PPyNT/P-Gr. The unmodified P-Gr showed the least response for the oxidation of catechol whereas PPyNT/P-Gr and $SrCuO_2$/PPyNT/P-Gr electrodes exhibit improved redox responses. Nevertheless, enzyme-modified electrode strikes the highest response of about 0.25 mA enumerating its enhanced electrocatalytic

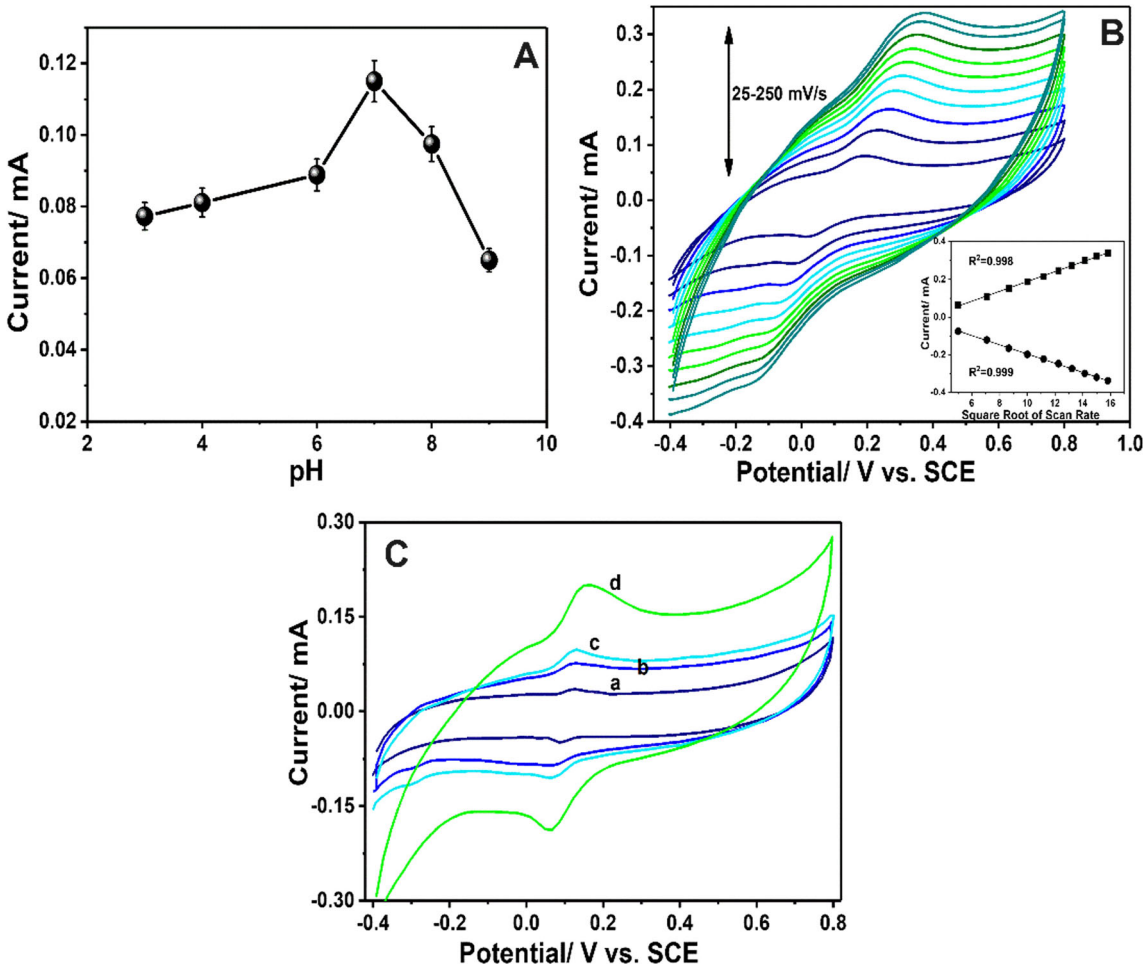

Fig. 4 **a** Effect of pH on PPO/$SrCuO_2$/PPyNT/P-Gr ($n = 5$). **b** CV of PPO/$SrCuO_2$/PPyNT/P-Gr for 10 μM catechol in 0.1 M PBS (pH = 7.0) with different scan rates (25, 50, 75, 100, 125, 150, 175, 200, 225, and 250 mV/s). Inset is the dependence of the redox peak current on the square root of scan rate. **c** CVs with 10 μM catechol in 0.1 M PBS (pH = 7.0) at 50 mV/s scan rate of a P-Gr, b PPyNT/P-Gr, c $SrCuO_2$/PPyNT/P-Gr, and d PPO/$SrCuO_2$/PPyNT/P-Gr

activity on the substrate, which points out to form promising enzyme immobilization matrix as well as fair transduction platform in the detection of catechol.

Electrochemical detection of catechol

The electrocatalytic redox reaction of the as-constructed sensor towards increasing concentration of catechol is examined using CV in oxygen saturated 0.1 M PBS (pH 7.0) within the potential range of − 0.4 V to 0.8 V at the scan rate of 50 mVs^{-1}. Figure 5 a displays the CV obtained at PPO/$SrCuO_2$/PPyNT/P-Gr for varying catechol concentrations. Evidently, the oxidation and reduction current has proportionally increased with the concentration of catechol in the linear range 1–15 μM, with the coefficient of regression (R^2) of 0.997 (inset of Fig. 5a). DPV is sensitive and high-resolution electrochemical technique run in the concentration range of catechol from 1 to 50 μM in 0.1 M PBS (pH = 7.0) in the potential window 0.65 V to − 0.1 V. The DPV results are shown in Fig. 5b. It is clear that the anodic peak current increases with the concentration of catechol. The inset of Fig. 5b authenticates direct proportionality of concentration of the analyte as a function of peak current with a coefficient of regression, R^2 of 0.992. Equations 1 and 2 are the plausible oxidation and reduction reactions occurring at PPO/$SrCuO_2$/PPyNT/P-Gr with catechol:

$$\text{Catechol} + O_2(PPO) \rightarrow 1,2\text{−Benzoquinone} + 2e^- \quad (1)$$

$$1,2\text{−Benzoquinone} + 2H^+ + 2e^- \rightarrow \text{Catechol} \quad (2)$$

The LOD and sensitivity of the proposed sensor are calculated from experimental data. The standard formulae suggested by IUPAC (2014a, b) accounts standard deviation (σ) of the blank run, slope (s) of the calibration curve (inset Fig. 5b), and surface area of the electrode. The calculated sensitivity and LOD are 15.60 μA μM^{-1} cm^{-2} and 0.15 μM respectively. Table 1 compares the analytical performance of the proposed sensor with recently reported ones to quantify

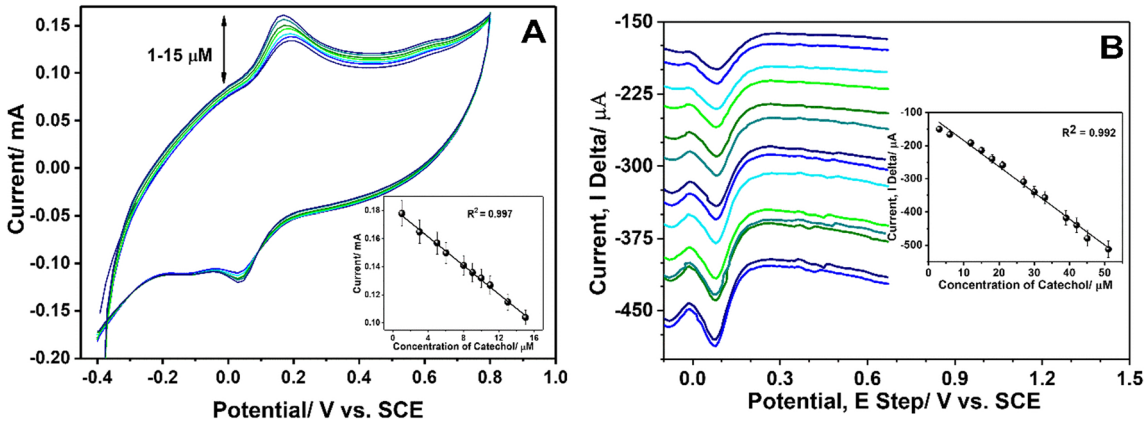

Fig. 5 **a** CV responses of PPO/$SrCuO_2$/PPyNT/P-Gr for different concentration (1 to 15 μM) of catechol in 0.1 M oxygen saturated PBS at 50 mV/s scan rate ($n = 5$). An inset shows the calibration curve for concentration (μM) as a function of peak current (mA). **b** DPV of PPO/$SrCuO_2$/PPyNT/P-Gr recorded for successive addition of increasing concentration (1–50 μM) of catechol in 0.1 M PBS (pH 7.0). The inset represents the calibration plot of peak current versus catechol concentration ($n = 5$)

catechol with varied matrices. Notably, the proposed PPO/$SrCuO_2$/PPyNT/P-Gr sensor has shown better analytical performance in terms of LOD to that reported in the literature (Table 1). With reference to reported catechol biosensors, the researchers have engaged a variety of engineered transducer matrices and enzymes to detect catechol. The matrices comprise of mainly metal-oxide nanomaterials, nano carbon allotropes, enzymes, conducting biopolymers, thin films, and noble metal nanoparticles which are expensive and involve critical synthesis protocols. In contrast, the present study has used a combination of perovskite micro-seeds and conductive biopolymer, synthesized facilely to constitute the transducer. PPO is used for selective and specific recognition of catechol in the system. The combined electrocatalytic behavior of PPO/$SrCuO_2$/PPyNT on P-Gr has made the as-developed senor promising for catechol detection and quantification.

Reproducibility, repeatability, and storage-stability of sensor

Repeatability and reproducibility are indeed crucial parameters to measure a sensor's field application. A set of six different PPO/$SrCuO_2$/PPyNT/P-Gr electrodes are prepared using the same protocol and tested for their response by CV for 10 μM catechol in 0.1 M PBS (pH = 7). Figure 6 a reveals that the current response is almost the same for each of the measurement recording an RSD of 0.76%. This makes the as-developed sensor suitable for the field applications.

Storage-stability of the sensor also referred to as shelf life (Nandini et al. 2014) is an essential factor to access the practical application of the developed sensor. It is investigated by measuring the response of sensor for 10 μM catechol in 0.1 M PBS (pH = 7) on every alternate day. The freshly prepared

Table 1 Comparison of proposed biosensor with reported sensor for catechol detection

Matrix	Linear Range (μM)	LOD (μM)	Reference
PPO/Agarose-guar gum	60–800	6.00	Tembe et al. (2007)
PPy/PPO	1–16	1.00	Ameer and Adeloju (2009)
MWCNT–NF–PMG film/GCE	30–1190	5.80	Umasankar et al. (2011)
Graphene doped CILE	10–300	0.70	Ma and Zhao (2012)
ITO/Sol–AuNPs	1-6	0.30	Singh et al. (2013)
Lac/AP/rGOs/Chit/GCE	15–700	7.00	Zhou et al. (2013)
CMWNTs-$NHCH_2CH_2NH_6$/GCE	5-80	1.00	Feng et al. (2014)
BG/GCE	1–75	0.20	Zhang et al. (2015)
Tyr-AuNPs-DHP/GCE	2.5–95	0.17	Vicentini et al. (2016)
Fc/APTMS/GO/GCE	3–112	1.10	Elancheziyan et al. (2017)
ZrO_2/Au	20–90	7.68	Bansal et al. (2017)
Cu/MOF-GN/GCE	1–1000	0.33	Li et al. (2018)
AuNPs/ZnO/Al_2O_3/GO,chit/GCE	0.5–40	3.10	Nazari et al. (2018)
PPO/$SrCuO_2$/PPyNT/P-Gr	1–50	0.15	This Work

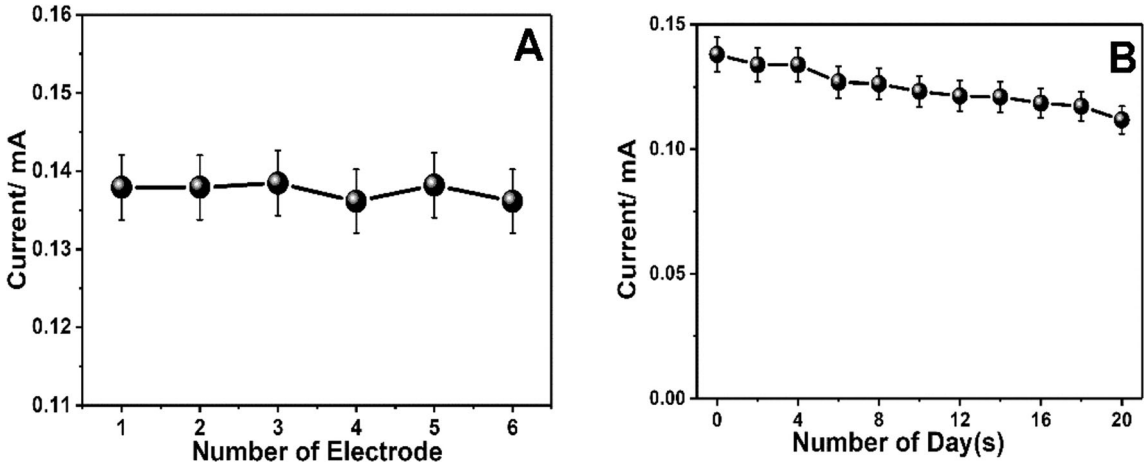

Fig. 6 **a** Peak current measured for10 μM catechol in 0.1 M PBS (pH = 7) with six individually modified PPO/$SrCuO_2$/PPyNT/P-Gr electrode to represent the sensor's repeatability ($n = 3$). **b** Storage-stability of PPO/$SrCuO_2$/PPyNT/P-Gr sensor ($n = 5$)

PBS is used to store the electrode at 4 °C. Figure 6 b shows the percentage decrease in the current response of PPO/$SrCuO_2$/PPyNT/P-Gr electrode. It is evident from the result that the developed sensor is reliable in the quantification of catechol for over 16–18 days with about 19% loss in signal (0.112 mA) as that of initial signal (0.138 mA). The electrode's high storability, reproducibility, and repeatability are ascribed to compatible and conducive microenvironment for nanomaterial and protein composite to constitute the sensor.

Effect of interferents

It is imperative that the wastewater and water samples have numerous organic and inorganic trace elements present along with the target analyte that can interfere in the functioning of the sensor. Therefore, the developed sensor is tested for the response along with the introduction of other usual interferons. Table 2 represents the change in current response (%) with 10 μM catechol when tenfold of interferons (SO_4^{-2}, NO_3^{-}, Zn^{+2}, Fe^{+3}, Ca^{2+}, and Mg^{2+}) spiked. The change in response ranges from − 3.5% to 2.7% of the initial response. Marginal signal drop is noted by the common interferons those commonly present in the water and wastewater. Hence, the present method is suitable for the sensitive detection of catechol in environmental samples.

Table 2 Study on interference by different species on 10 μM catechol

SL	Interferons	Volume spiked in μM	Change in current (%)
1	SO_4^{-2}	100	− 0.5
2	NO^{-3}	100	1.2
3	Zn^{+2}	100	2.6
4	Fe^{+3}	100	1.9
5	Ca^{+2}	100	2.0
6	Mg^{+2}	100	− 1.3
7	SO_4^{-2}	100	0.6

Real sample analysis

Finally, the PPO/$SrCuO_2$/PPyNT/P-Gr probe is tested for detection of catechol in the real environmental samples, individually in mineral water (bottled), tap water (in-house), and domestic wastewater. In the study, the PBS is diluted with real samples in equal proportion followed by spiking known amount of catechol. Mineral water, tap water, and domestic wastewater are used for the study after filtering with Whatman Grade 1 filter paper. The CV measured quantities found and percentage recovery is calculated. Table 3 shows the recovery of the target from different samples. The recovery is as high as 99.6% in mineral water and minimum of 93.6% in domestic wastewater. Table 3 is instrumental to remark on the efficiency of the proposed sensor for quantification of catechol in water and wastewater.

Table 3 Determination of catechol by PPO/$SrCuO_2$/PPyNT/P-Gr in real samples

SN	Sample	Catechol spiked (in μM)	Found (in μM)	Recovery (%)	RSD (%)
1	Mineral water	50	49.8	99.6	1.132
2		50	48.7	97.4	
3		50	49.1	98.2	
4	Tap water	50	47.6	95.2	0.435
5		50	48	96.0	
6		50	47.9	95.8	
7	Domestic	50	47.1	94.2	0.535
8	wastewater	50	46.8	93.6	
9		50	47.3	94.6	

Conclusions

Accentuating the threat from phenolic pollutants in the environmental samples, the present work proposes enzyme-based biosensor, PPO/$SrCuO_2$/PPyNT/P-Gr, for the quantification of catechol. The developed sensor is demonstrative of the synergy of tailored micro-perovskite, promising polypyrrole, highly selective enzyme, and the economical electrode. Specifically, the study explored a new electrode matrix validated for electrochemical detection of catechol. $SrCuO_2$, one among the new perovskite compounds, is exploited for its electrocatalytic capability as transducer constituent. The synthesis of PPyNT with methyl orange template is rare of its kind and facile, which readily exhibits compatibility with $SrCuO_2$ to act as transducer of the biosensor. The PPO enzyme is successfully extracted from a newer source, *Ipomoea batatas*, to perform the biorecognition of catechol. Further, the matrix of $SrCuO_2$ and PPyNT played a significant role in embedding the enzyme and improving the conductivity of the electrode. Use of pencil graphite electrode is pivotal in the study that showed fair electrochemical sensitivity over other carbon-based electrodes and are easily available material in the markets. The characteristic combination of new transducer matrix and PPO enzyme has assured reliability and economy of the sensor over other catechol sensors. In addition, the real sample analysis predicts on potential "on-site" performance of the sensor. The reproducibility and stability of proposed bioelectrode is on par with most of the prior reported ones. Hence, the as-fabricated sensor accents its candidature towards analytics owning to its decisive performance factors.

Acknowledgments The authors gratefully acknowledge the support from Department of Chemistry and Department of Environmental Engineering of JSS Science and Technology University, Mysuru, Karnataka, India.

References

Ameer Q, Adeloju SB (2009) Development of a potentiometric catechol biosensor by entrapment of tyrosinase within polypyrrole film. Sensors Actuators B Chem 140:5–11. https://doi.org/10.1016/j.snb.2009.03.056

Arfin T, Rangari SN (2018) Graphene oxide-ZnO nanocomposite modified electrode for the detection of phenol. Anal Methods 10:347–358. https://doi.org/10.1039/c7ay02650a

Aziz AA, Yong KS, Ibrahim S, Pichiah S (2012) Enhanced magnetic separation and photocatalytic activity of nitrogen doped titania photocatalyst supported on strontium ferrite. J Hazard Mater 199–200:143–150. https://doi.org/10.1016/j.jhazmat.2011.10.069

Balasubramanian P, Balamurugan TST, Chen SM, Chen TW (2017) Facile synthesis of orthorhombic strontium copper oxide microflowers for highly sensitive nonenzymatic detection of glucose in human blood. J Taiwan Inst Chem Eng 81:182–189. https://doi.org/10.1016/j.jtice.2017.10.040

Bansal P, Bhanjana G, Prabhakar N, Dhau JS, Chaudhary GR (2017) Electrochemical sensor based on ZrO_2 NPs/Au electrode sensing layer for monitoring hydrazine and catechol in real water samples. J Mol Liq 248:651–657. https://doi.org/10.1016/j.molliq.2017.10.098

David IG, Badea IA, Radu GL (2013) Disposable carbon electrodes as an alternative for the direct voltammetric determination of alkyl phenols from water samples. Turk J Chem 37:91–100. https://doi.org/10.3906/kim-1203-49

Elancheziyan M, Manoj D, Saravanakumar D, Thenmozhi K, Senthilkumar S (2017) Amperometric sensing of catechol using a glassy carbon electrode modified with ferrocene covalently immobilized on graphene oxide. Microchim Acta 184:2925–2932. https://doi.org/10.1007/s00604-017-2312-2

Fartas FM, Abdullah J, Yusof NA et al. (2017) Biosensor based on tyrosinase immobilized on graphene-decorated gold nanoparticle/chitosan for phenolic detection in aqueous. Sensors (Switzerland) 17. https://doi.org/10.3390/s17051132

Feng S, Zhang Y, Zhong Y, Li Y, Li S (2014) Simultaneous determination of hydroquinone and catechol using covalent layer-by-layer self-assembly of carboxylated-MWNTs. J Electroanal Chem 733:1–5. https://doi.org/10.1016/j.jelechem.2014.09.019

Gul I, Ahmad MS, Naqvi SMS et al (2017) Polyphenol oxidase (PPO) based biosensors for detection of phenolic compounds: a review. J Appl Biol Biotechnol 5:72–85. https://doi.org/10.7324/JABB.2017.50313

Han WK, Choi JW, Hwang GH, Hong SJ, Lee JS, Kang SG (2006) Fabrication of Cu nano particles by direct electrochemical reduction from CuO nano particles. Appl Surf Sci 252:2832–2838. https://doi.org/10.1016/j.apsusc.2005.04.049

IUPAC (2014a) Limit of detection in analysis, 2nd edn. Blackwell Scientific Publications, Oxford. https://doi.org/10.1351/goldbook.L03540

IUPAC (2014b) Sensitivity in metrology and analytical chemistry, A, 2nd edn. Blackwell Scientific Publications, Oxford. https://doi.org/10.1351/goldbook.S05606

Khorsandi H, Gholizadeh M, Aghapour A ahmad (2018) Catechol biodegradation by a novel hybrid anoxic biofilter. Environ Technol 1–8. https://doi.org/10.1080/09593330.2018.1510434

Kopecky D, Skodova J, Vrnata M, Fitl P (2012) Polypyrrole micro/nanostructure prepared using azo dyes with different substituents. Adv Mater Phys Chem 02:89–91. https://doi.org/10.4236/ampc.2012.24B024

Kopecký D, Varga M, Prokeš J, Vrňata M, Trchová M, Kopecká J, Václavík M (2017) Optimization routes for high electrical conductivity of polypyrrole nanotubes prepared in presence of methyl orange. Synth Met 230:89–96. https://doi.org/10.1016/j.synthmet.2017.06.004

Li H, Hu X, Zhu H et al (2017) Amperometric phenol biosensor based on a new immobilization matrix: Polypyrrole nanotubes derived from methyl orange as dopant. Int J Electrochem Sci 12:6714–6728. https://doi.org/10.20964/2017.07.80

Li J, Xia J, Zhang F, Wang Z, Liu Q (2018) An electrochemical sensor based on copper-based metal-organic frameworks-graphene composites for determination of dihydroxybenzene isomers in water. Talanta 181:80–86. https://doi.org/10.1016/j.talanta.2018.01.002

de Lima F, Lucca BG, Barbosa AMJ, Ferreira VS, Moccelini SK, Franzoi AC, Vieira IC (2010) Biosensor based on pequi polyphenol oxidase immobilized on chitosan crosslinked with cyanuric chloride for thiodicarb determination. Enzym Microb Technol 47:153–158. https://doi.org/10.1016/j.enzmictec.2010.05.006

Liu Z, Zhang Y, Bian C, Xia T, Gao Y, Zhang X, Wang H, Ma H, Hu Y, Wang X (2019) Highly sensitive microbial biosensor based on recombinant Escherichia coli overexpressing catechol 2,3-dioxygenase for reliable detection of catechol. Biosens Bioelectron 126:51–58. https://doi.org/10.1016/J.BIOS.2018.10.050

Ma L, Zhao G-C (2012) Simultaneous determination of hydroquinone, catechol and resorcinol at graphene doped carbon ionic liquid

electrode. Int J Electrochem 2012:1–8. https://doi.org/10.1155/2012/243031

Maringa A, Mugadza T, Antunes E, Nyokong T (2013) Characterization and electrocatalytic behaviour of glassy carbon electrode modified with nickel nanoparticles towards amitrole detection. J Electroanal Chem 700:86–92. https://doi.org/10.1016/j.jelechem.2013.04.022

Nandini S, Nalini S, Sanetuntikul J, Shanmugam S, Niranjana P, Melo JS, Suresh GS (2014) Development of a simple bioelectrode for the electrochemical detection of hydrogen peroxide using Pichia pastoris catalase immobilized on gold nanoparticle nanotubes and polythiophene hybrid. Analyst 139:5800–5812. https://doi.org/10.1039/c4an01262c

Nazari M, Kashanian S, Moradipour P, Maleki N (2018) A novel fabrication of sensor using ZnO-Al_2O_3ceramic nanofibers to simultaneously detect catechol and hydroquinone. J Electroanal Chem 812:122–131. https://doi.org/10.1016/j.jelechem.2018.01.058

Sandeep S, Santhosh AS, Swamy NK, Suresh GS, Melo JS, Nithin KS (2018a) Electrochemical detection of L-dopa using crude polyphenol oxidase enzyme immobilized on electrochemically reduced RGO-Ag nanocomposite modified graphite electrode. Mater Sci Eng B Solid-State Mater Adv Technol 232–235:15–21. https://doi.org/10.1016/j.mseb.2018.10.014

Sandeep S, Santhosh AS, Swamy NK, Suresh GS, Melo JS, Chamaraja NA (2018b) A biosensor based on a graphene nanoribbon/silver nanoparticle/polyphenol oxidase composite matrix on a graphite electrode: application in the analysis of catechol in green tea samples. New J Chem 42:16620–16629. https://doi.org/10.1039/C8NJ02325E

Singh S, Jain DVS, Singla ML (2013) Sol-gel based composite of gold nanoparticles as matix for tyrosinase for amperometric catechol biosensor. Sensors Actuators B Chem 182:161–169. https://doi.org/10.1016/j.snb.2013.02.111

Swamy NK, Sandeep S, Santhosh AS (2017) Conductive polymers and their nanohybrid transducers for electrochemical biosensors applications : a brief review. J Adv Chem Sci S2:6–9. https://doi.org/10.22607/IJACS.2017.S02002

Tembe S, Inamdar S, Haram S, Karve M, D'Souza SF (2007) Electrochemical biosensor for catechol using agarose-guar gum entrapped tyrosinase. J Biotechnol 128:80–85. https://doi.org/10.1016/j.jbiotec.2006.09.020

Trchová M, Stejskal J (2018) Resonance Raman spectroscopy of conducting polypyrrole nanotubes: disordered surface versus ordered body. J Phys Chem A 122:9298–9306. https://doi.org/10.1021/acs.jpca.8b09794

Umasankar Y, Periasamy AP, Chen SM (2011) Electrocatalysis and simultaneous determination of catechol and quinol by poly(malachite green) coated multiwalled carbon nanotube film. Anal Biochem 411:71–79. https://doi.org/10.1016/j.ab.2010.12.002

Usai V, Mugadza T, Chigondo F, Shumba M, Nharingo T, Moyo M, Tshuma P (2019) Synthesis and characterisation of cobalt oxide nanoparticles decorated graphene oxide and its electrocatalytic behaviour. Polyhedron 157:192–199. https://doi.org/10.1016/j.poly.2018.10.002

Vicentini FC, Garcia LLC, Figueiredo-Filho LCS et al (2016) A biosensor based on gold nanoparticles, dihexadecylphosphate, and tyrosinase for the determination of catechol in natural water. Enzym Microb Technol 84:17–23. https://doi.org/10.1016/j.enzmictec.2015.12.004

Wang HF, Wu YY, Yan XP (2013) Room-temperature phosphorescent discrimination of catechol from resorcinol and hydroquinone based on sodium tripolyphosphate capped Mn-doped ZnS quantum dots. Anal Chem 85:1920–1925. https://doi.org/10.1021/ac303374s

Yan Y, Wu X, Zhang H (2016) Catalytic wet peroxide oxidation of phenol over Fe_2O_3/MCM-41 in a fixed bed reactor. Sep Purif Technol 171:52–61. https://doi.org/10.1016/j.seppur.2016.06.047

Yang X, Zhu Z, Dai T, Lu Y (2005) Facile fabrication of functional polypyrrole nanotubes via a reactive self-degraded template. Macromol Rapid Commun 26:1736–1740. https://doi.org/10.1002/marc.200500514

Yashas SR, Shivakumara BP, Udayashankara TH, Krishna BM (2018) Laccase biosensor: green technique for quantification of phenols in wastewater (a review). Orient J Chem 34:631–637. https://doi.org/10.13005/ojc/340204

Yogita KV et al (2016) Phenols & phenolic compounds. Newsletter, CPCB, India Available from: http://cpcb.nic.in/uploads/News_Letter_Phenols_Phenolic_Compounds_2017.pdf. Accessed August 2016

Yousefi R, Jamali-Sheini F, Cheraghizade M, Khosravi-Gandomani S, Sáaedi A, Huang NM, Basirun WJ, Azarang M (2015) Enhanced visible-light photocatalytic activity of strontium-doped zinc oxide nanoparticles. Mater Sci Semicond Process 32:152–159. https://doi.org/10.1016/j.mssp.2015.01.013

Zeng G, Zhu Y, Zhang Y, Zhang C, Tang L, Guo P, Zhang L, Yuan Y, Cheng M, Yang C (2016) Electrochemical DNA sensing strategy based on strengthening electronic conduction and a signal amplifier carrier of nanoAu/MCN composited nanomaterials for sensitive lead detection. Environ Sci Nano 3:1504–1509. https://doi.org/10.1039/c6en00323k

Zhang Y, Sun R, Luo B, Wang L (2015) Boron-doped graphene as high-performance electrocatalyst for the simultaneously electrochemical determination of hydroquinone and catechol. Electrochim Acta 156:228–234. https://doi.org/10.1016/j.electacta.2014.12.156

Zhou XH, Liu LH, Bai X, Shi HC (2013) A reduced graphene oxide based biosensor for high-sensitive detection of phenols in water samples. Sensors Actuators B Chem 181:661–667. https://doi.org/10.1016/j.snb.2013.02.021

Zhu Y, Zeng GM, Zhang Y, Tang L, Chen J, Cheng M, Zhang LH, He L, Guo Y, He XX, Lai MY, He YB (2014) Highly sensitive electrochemical sensor using a MWCNTs/GNPs-modified electrode for lead (II) detection based on Pb^{2+}-induced G-rich DNA conformation. Analyst 139:5014–5020. https://doi.org/10.1039/c4an00874j